

## Thermally activated dynamic bonding network for enhancing high-temperature energy storage performance of PEI-based dielectrics

Jialong Li, Xiaoxu Liu\*, Bingshun Huang, Dongyang Chen, Zhaoru Chen, Yanpeng Li, Yu Feng, Jinghua Yin, Haozhe Yi, Taoqi Li

### Supporting Information

#### *Supplemented Experimental/Methods Section*

##### *Materials*

Zinc acetate dihydrate ( $\text{Zn}(\text{CH}_3\text{COO})_2$ ), 2-methylimidazole and cetyltrimethyl ammonium bromide used for synthesizing the Zif-8 MOFs were purchased from Sigma Aldrich. For preparing the pristine PEI and their composites, 1-methyl-2-pyrrolidinone (NMP), 4,4'-diaminodiphenyl ether (ODA) and 4,4'-isopropylidenediphenoxy bis-(phthalic anhydride) (BPADA) were purchased from Sinopharm Chemical Reagent Co., Ltd. These materials were used without any further purification.

##### *Preparation of MOFs and the PEI-based composites*

The zeolitic imidazolate framework-8 (Zif-8, a typical MOF) were synthesized through using the typical solvothermal method<sup>1</sup>. The multidentate bonded PEI/MOFs composite films were prepared by using in-situ polymerization process, as shown in Figure S1. Firstly, the weighted MOFs (0.2, 0.5, 1 and 3 wt%) were dispersed into 18 ml NMP with the assistance of ultrasonication in the three-necked flask, following 1.5g ODA were dissolved into the solution. Then added 4.0 g BPADA powder into the flask per hour 1.0 g to obtain the PEI precursor. The solution casting method is adopted to prepare the composite films after the bubble in the flask disappeared completely, the thickness is controlled at 10-12  $\mu\text{m}$ . Subsequently, the sample was held in the vacuum oven at 80 °C overnight to evaporate the NMP solvent. Then rising the temperature of the vacuum oven by 60 °C per hour, the specific temperatures are 140, 200, 260 and 320 °C. The PEI-based composites can be obtained after this gradient thermal imidization process.

During the preparation of ZIF-8 MOFs, due to the escape of guest molecules, the volatilization of organic solvents and the deletion of ligands, a large amount of Zn open metal sites (OMSs) would expose to the MOFs surface<sup>2</sup>. In this work, the 4,4'-diaminodiphenyl ether (ODA) is used as the one of the monomers to synthesize PEI. The  $-\text{NH}_2$  group at the tail of

ODA could provide abundant H<sup>+</sup>, which could coordinatively bond with the Zn OMSs of MOFs. Our previous work has scientifically verified this result in the polyimide-based system<sup>3</sup>. Therefore, the specific structure which is similar to the covalent crosslinking network is named as “multisite bonding network”.

### *Characterization*

The morphology of the MOFs and the cross-section image of the PEI/MOFs composites were observed by via using scanning electron microscope (SEM, *shanghai*). The X-ray diffraction (XRD) patterns of the MOFs and the PEI-based composites were recorded by a Smart Lab 9kW equipment. The chemical construction and elemental composition of both the MOFs and the PEI/MOFs composites were characterized by the Fourier transform infrared spectrometer (FT-IR, Bruker Vector-22) and the X-ray photoelectron spectroscopy (XPS, Axis Supra), respectively. The DSC&TGA analysis of the Zif-8 MOFs were performed on a TA-Q600 synchronous thermal analysis system. Dynamic mechanical analysis (DMA) of the PEI-based composites was operated on a DMA analyzer (NETZSCH DMA 242) in the stretch mode, the oscillation frequency is 1 Hz. Testing temperature ranged from room temperature to 300 °C at a heating rate of 3 °C min<sup>-1</sup>. Small angle X-ray scattering (SAXS) of the composites were carried out at the beam line 1W2A in Beijing Synchrotron Radiation Facility (BSRF). The storage ring was operated at 2.5 GeV with a current of ~80 mA. A charged coupled device type Mar165-CCD was used to collect 2D scattering patterns with the sample-to-detector distance in the direction of the beam is 1900 mm. The in-situ X-ray absorption fine structure (XAFS) spectra of Zn *K*-edge were measured at the XAFS station of beamline 1W1B of BSRF in transmission mode. The samples (3 cm × 2 cm) were soaked in NMP for 3 days to performe the solubility test. The treated samples were rinsed with deionized water and then immersed in hot methanol after they were dried entirely.

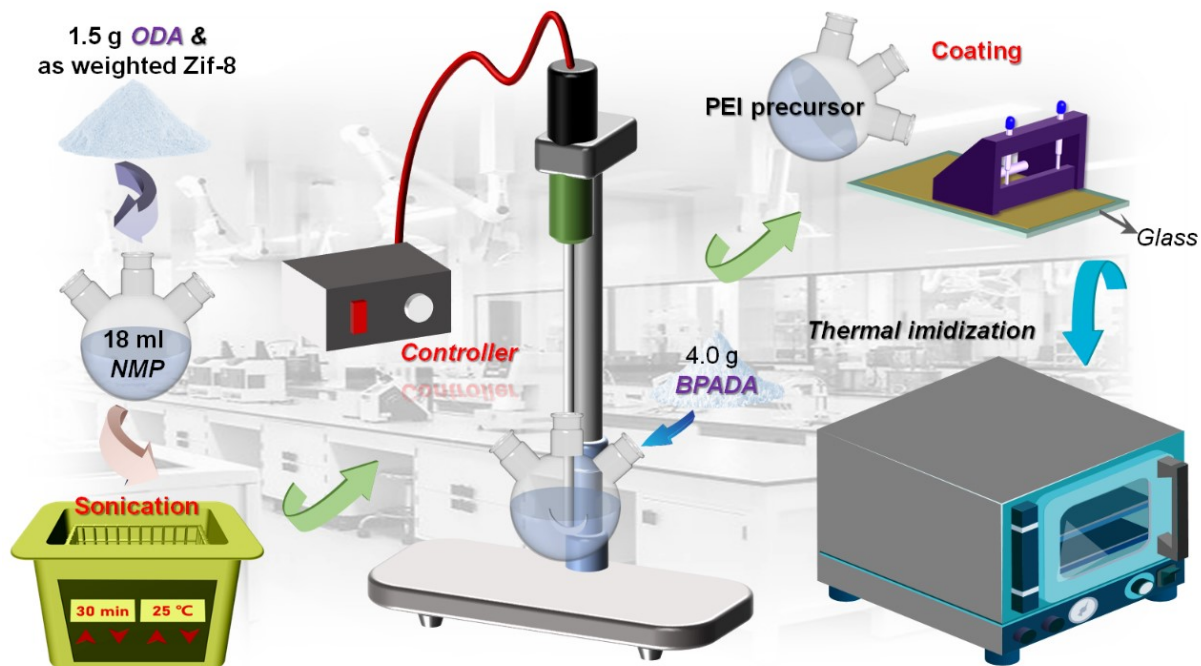


**Figure S1.** Schematic illustration for the synthesis of the PEI/MOFs composites.

#### *Performance Measurements of the PEI/MOFs composites*

The dielectric constant ( $\epsilon_r$ ), dielectric loss ( $\tan\delta$ ) and electric modulus of the composites were tested through using a Concept 40 broadband dielectric spectrometer. For the frequency-depended dielectric performance of the composites, the measurements were performed at room temperature with the frequency ranges from  $10^1$  to  $10^7$  Hz. For the temperature-depended measurements, the operating temperature is set to be 30-200 °C. Breakdown strength ( $E_b$ ) and the electric polarization-electric field ( $P$ - $E$ ) loops of the PEI-based composites were carried out by using a *Poly-k* ferroelectric test system at 10 Hz at both room temperature and high temperature. The energy storage density ( $U_e$ ) and related energy storage efficiency ( $\eta$ ) of the composites were calculated according to the measured  $P$ - $E$  loops. 10 mm and 3 mm golden electrodes were vacuum-evaporated onto both sides of the samples before the dielectric performance and  $E_b$  measurements, respectively. 3 mm, 5 mm and 7 mm electrodes were evaporated on the composites surface for the  $P$ - $E$  loops measurements.

#### *Supplemented results*

The SEM image of the Zif-8 MOFs are shown in Figure S2(a), the enlarged SEM image in Figure S2(b) indicates the Zif-8 present typical truncated rhombic dodecahedral (TRD) structure. Meanwhile, the size of the Zif-8 concentrated on about 300-370 nm (Figure S2(c)), which is due to the less-reactive zinc acetate dihydrate is used as salts in synthesizing the Zif-8, the results are in great coincidence with previous literature <sup>1</sup>.

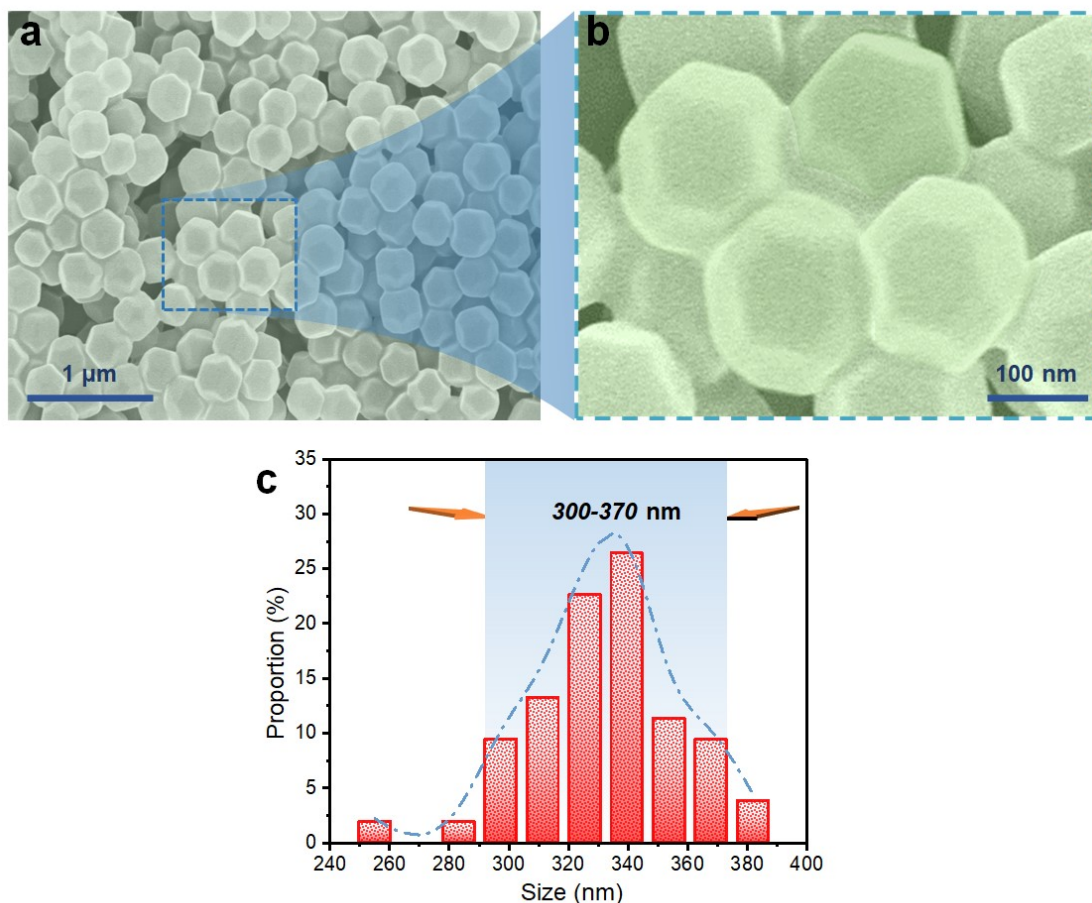


**Figure S2.** (a) SEM and (b) high-resolution SEM image of the Zif-8 MOFs and (c) their size distribution.

The XRD pattern of the Zif-8 is shown in Figure S3(a), the diffraction peaks at 7.8 °, 10.8 °, 13.1 °, 15.2 ° and 18.4 ° correspond to the (011), (002), (112), (022) and (222) planes of typical Zif-8 MOFs. The FT-IR spectrum of the synthesized MOFs at wavenumber of 993  $\text{cm}^{-1}$ , 1143  $\text{cm}^{-1}$ , 1587  $\text{cm}^{-1}$  and 2927  $\text{cm}^{-1}$ , 3136  $\text{cm}^{-1}$  are in agreement of the C-N, C=N and C-H bonds of Zif-8, as shown in Figure S3(b).

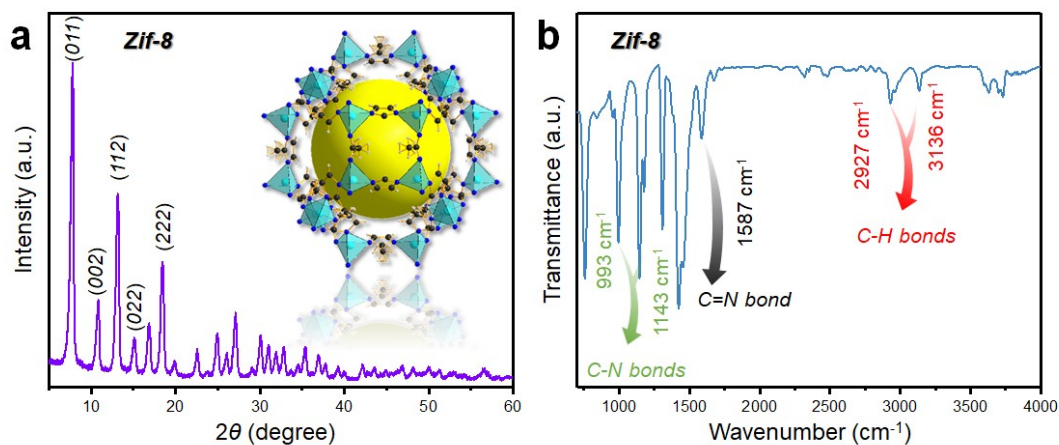


**Figure S3.** (a) XRD pattern and (b) FT-IR spectrum of the Zif-8 MOFs.

The TG analysis of the prepared MOFs shows a gradual weight loss of 15.03% at about 35 to 200 °C is due to the volatilization of guest molecules (*e.g.* H<sub>2</sub>O) and residual solvents in Zif-8 MOFs. Following a plateau started at ~420 °C is consistent with the framework decomposition of Zif-8 MOFs<sup>2</sup>, as presented in Figure S4. Besides, an obvious endothermic peak of the prepared MOFs starts to appear at ~420 °C in its DSC curve, which suggested that the MOFs start to decompose and transform into ZnO at this stage<sup>4</sup>. It is mentionable that the highest temperature of thermal imidization process for the PEI/MOFs composites is 320 °C. The thermal imidization of the PEI-based composites does not cause the decomposition of MOFs. Moreover, the removal of guest molecules and residual solvents could endow the MOFs with high crystalline properties, which might enhance the comprehensive performances of the PEI/MOFs composites<sup>3</sup>.

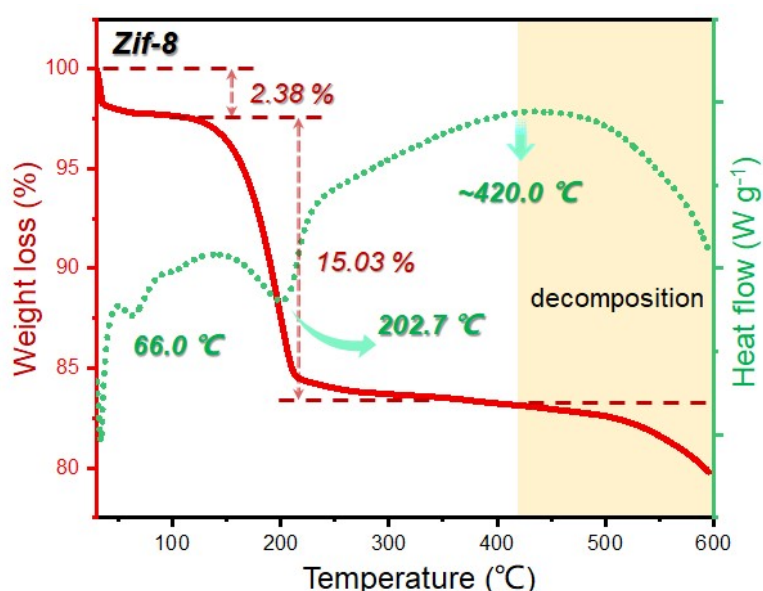


**Figure S4.** TGA&DSC analysis of Zif-8 MOFs.

The XPS results of the synthesized MOFs clearly indicate the appearance of the C, N, O and Zn elements, as shown in Figure S5. All these results indicate the successful synthesis of the Zif-8 MOFs.

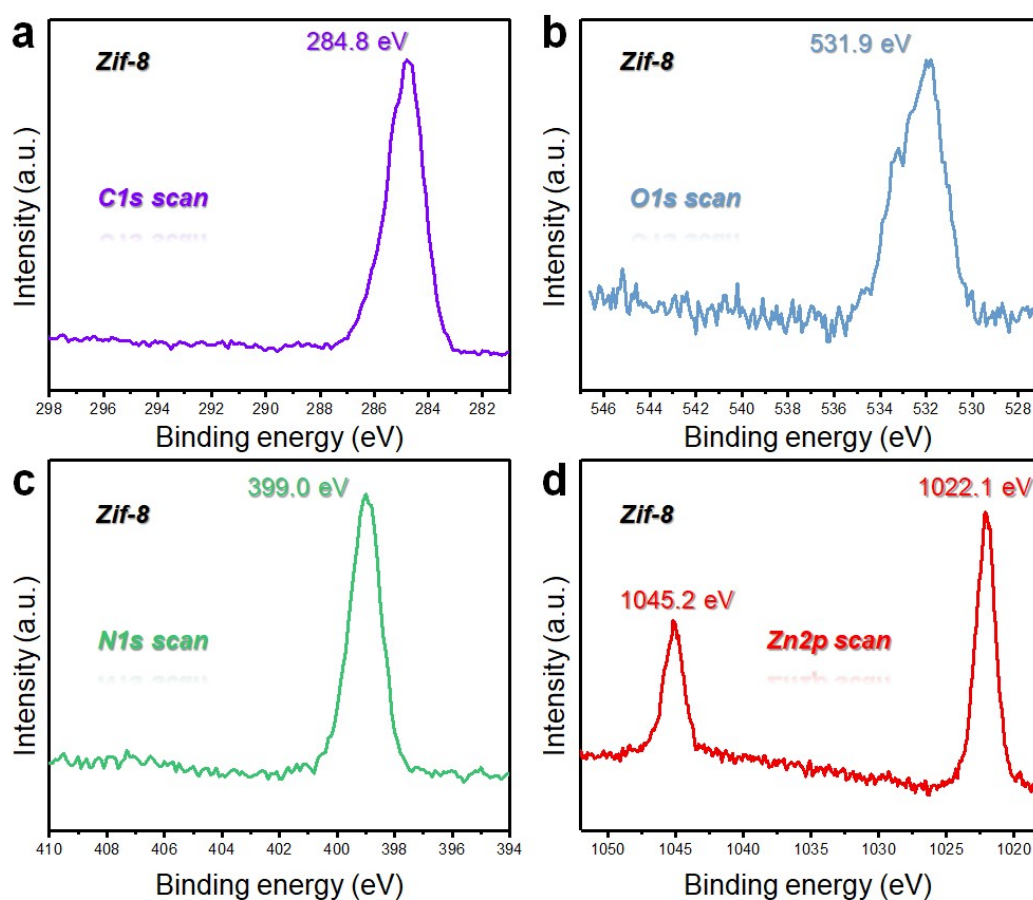


**Figure S5.** XPS spectra of the Zif8: (a) C 1s, (b) O 1s, (c) N 1s and (d) Zn 2p core-level spectra.



**Figure S6.** Macroscopic photo of the PEI/Zif-8 composites.

As shown in Figure S7, only few amounts of intact MOFs can be observed in the cross-section image of the PEI/MOFs composite. Owing to the PEI chains interspersed in the pores of the MOFs would coordinatively bonded with the Zn OMS in MOFs, finally generate the multisite bonding networks within the composites. Most MOFs lose their original morphology

after this process, and exist in the composite as portions of the multisite bonding networks. Consequently, the MOFs are difficult to be observed while the Zn element nearly distribute in the whole material. This phenomenon indicates the successfully construction of the multisite bonding networks within the PEI-based composites.

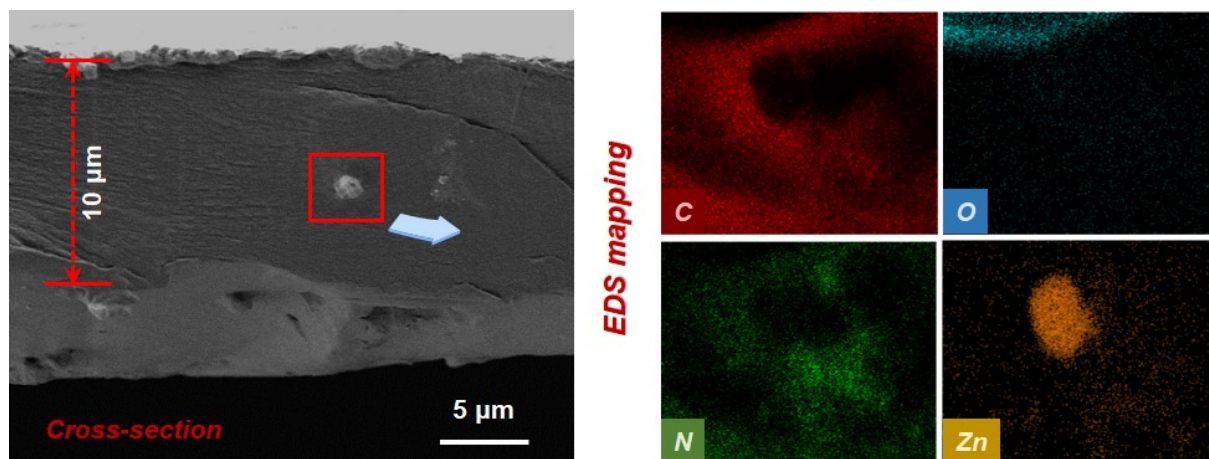


**Figure S7.** Cross-section SEM image of the PEI-based composites containing 1 wt% MOFs and the related elemental mapping images of C, O, N and Zn elements.

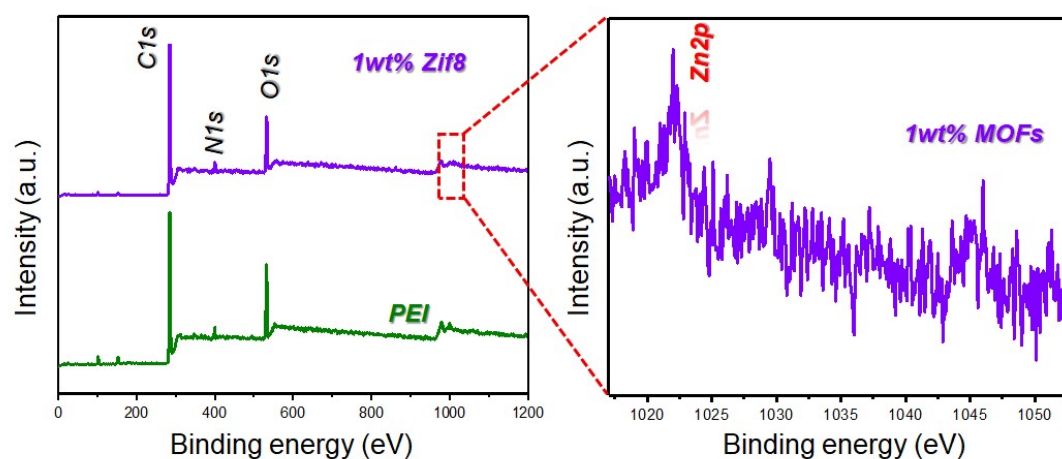


**Figure S8.** Overall XPS spectra of the PEI and the PEI/MOFs composites and Zn 2p core-level spectra of the PEI/Zif-8 composites.

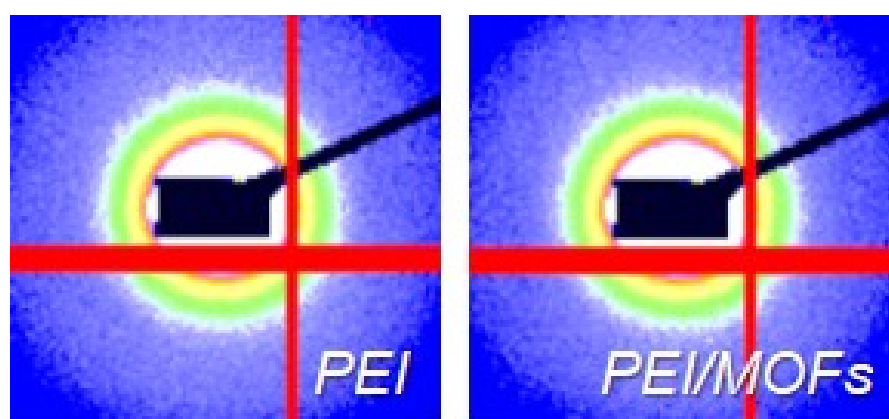


**Figure S9.** The original 2D SAXS images of PEI and the PEI/MOFs composites.

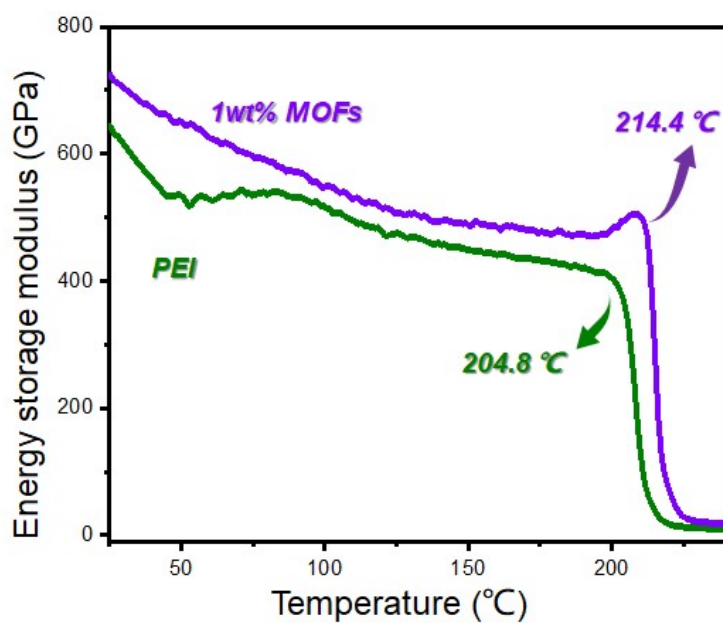


**Figure S10.** The energy storage modulus ( $E'$ ) of PEI and the PEI/MOFs composite.

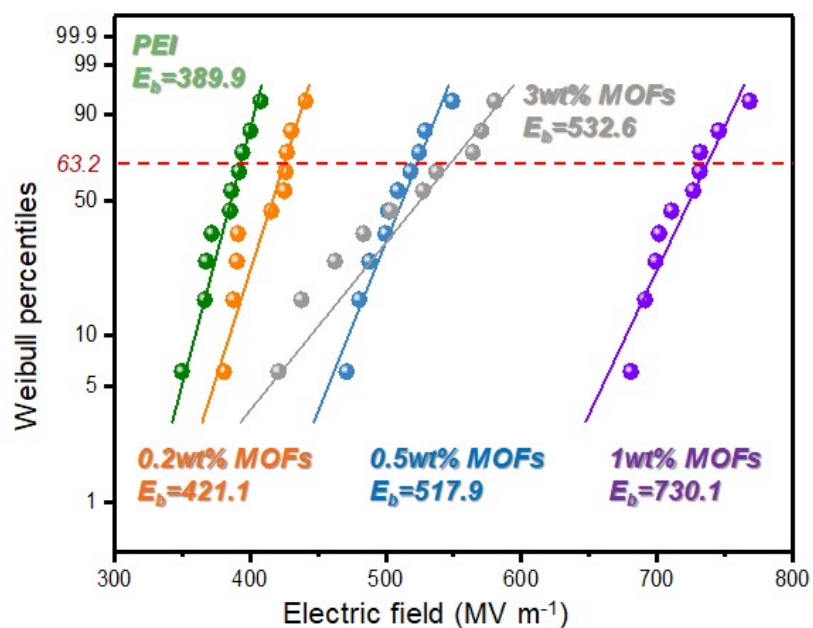


**Figure S11.** Weibull breakdown strength ( $E_b$ ) of PEI and the PEI/MOFs composites at room temperature.

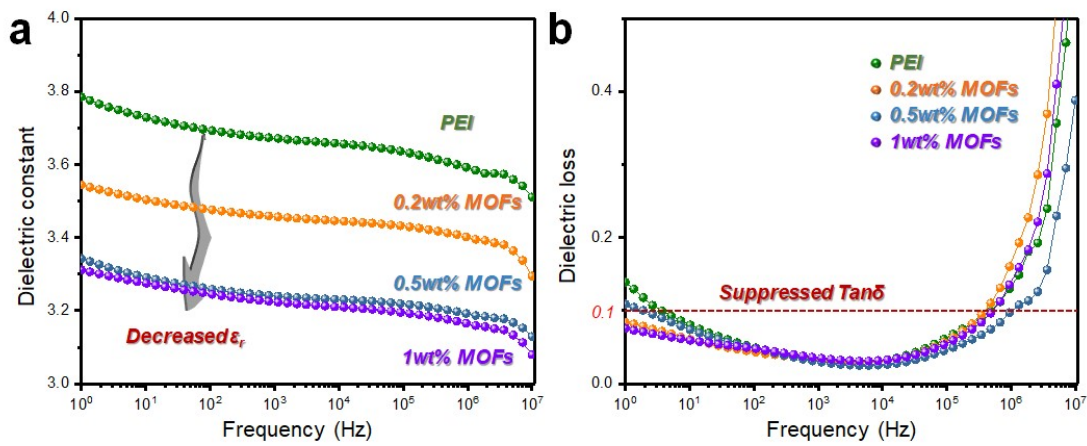


**Figure S12.** Frequency dependence of (a) dielectric constant ( $\epsilon_r$ ) and (b) dielectric loss (Tan $\delta$ ) of PEI and the PEI/MOFs composites.

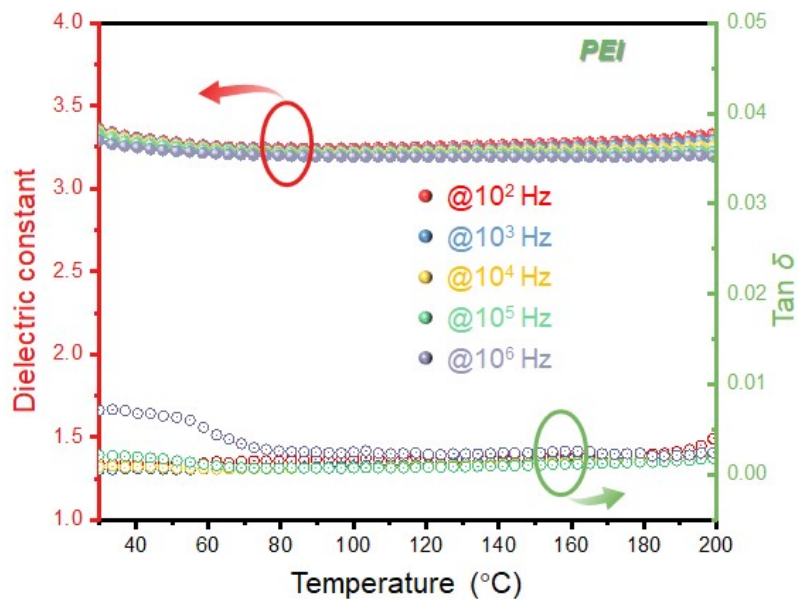


**Figure S13.** Temperature dependence of dielectric constant ( $\epsilon_r$ ) and dielectric loss tangent (Tan $\delta$ ) of the PEI.

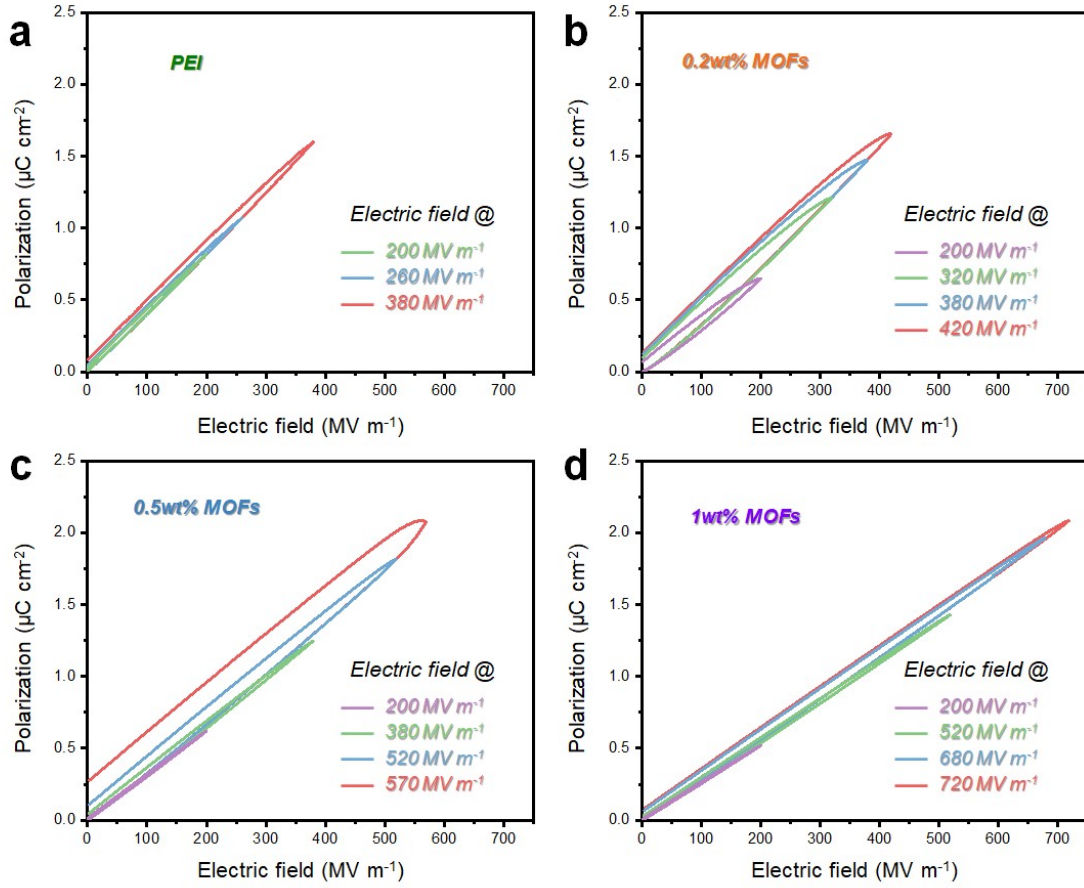


**Figure S14.** *P-E* loops of the PEI and PEI/MOFs composites at different MOFs loading.

The energy storage density ( $U_e$ ) and charge-discharge efficiency ( $\eta$ ) of the PEI-based the composites were calculated through the *P-E* loops according to Eq. S1 and S2.

$$U_e = \int_{D_r}^{D_{max}} E dD, D = P + \epsilon_0 E \quad \text{Eq. S1}$$

$$\eta = \frac{U_e}{\int_0^{D_{max}} E dD} \quad \text{Eq. S2}$$

where  $\epsilon_r$  is the dielectric constant of the material,  $E$  is the applied electric field,  $D$  is the electric displacement,  $P$  is the polarization,  $\epsilon_0 = 8.85 \times 10^{-12} \text{ F m}^{-1}$  is the dielectric constant of vacuum.  $D_{max}$  and  $D_r$  are the maximum and remnant electric displacement corresponding to the maximum and remnant polarization ( $P_{max}$  and  $P_r$ ).

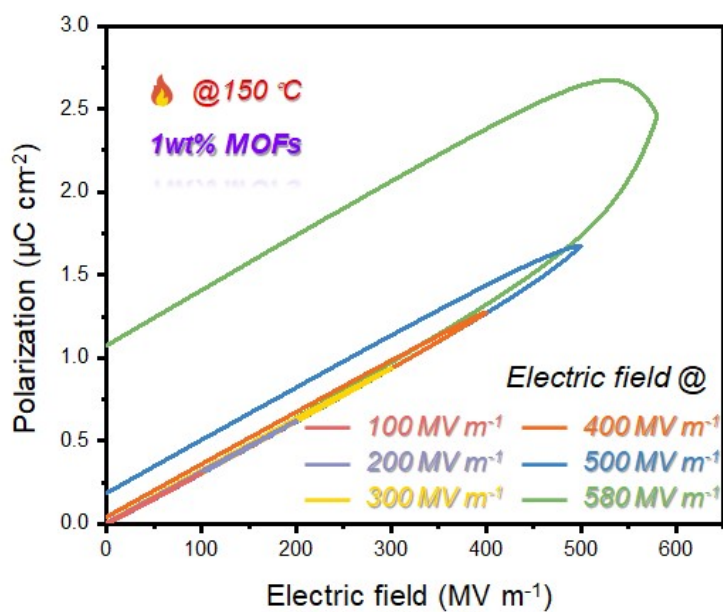


**Figure S15.** *P-E* loops of the PEI/MOFs composites at 150 °C.

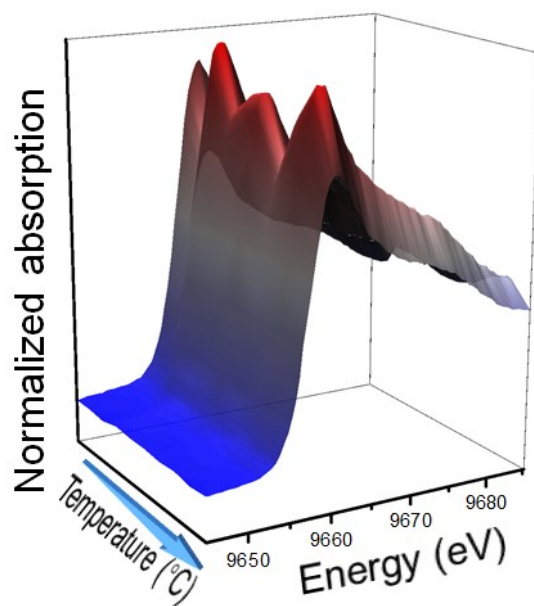


**Figure S16.** Normalized Zn *K*-edge XANES spectra of the PEI/MOFs composites from *RT* to 150 °C.

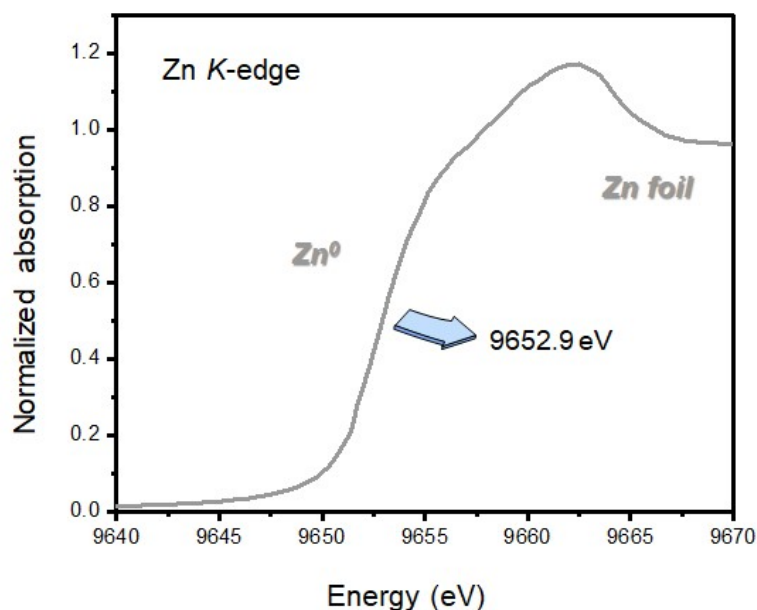


**Figure S17.** Normalized Zn K-edge XANES spectra of Zn foil.

The model of single PEI polymer chain was constructed by dehydration polymerization of BPADA and ODP. According to the characterization results and our previous work<sup>3</sup>, the multidentate bonded model of single PEI/Zif-8 chain was established after optimization, as shown in Figure S18. To build the model the pristine PEI and the PEI/Zif-8 composite, 20 copies of the single model of PEI and PEI/Zif-8 chain were made, respectively. Then these polymer chains were randomly placed in the space frame in a gaseous manner. The pressure and temperature were set to be 0.4 GPa and 273 K, and pressing the gas cube. After one dynamic calculation, the pressure was released to be 0 MPa, the stable solid models of the pristine PEI and PEI/Zif-8 composites can be obtained.

The molecular dynamics calculations of these solid models were performed at different temperatures, the intermolecular binding energy between PEI and PEI/Zif-8 chains can be attained. The force field is COMPASS II. In order to obtain a stable density structure, NPT is selected in the ensemble, the step size is set to 1 fs, and the total simulation time is 50.0 ps for every temperature or every pressure.

The electrostatic potential around the PEI/Zif-8 multidentate bonded chain was calculated via using the semiempirical quantum chemistry method. The red or blue region denotes the negative or positive electrostatic potential area, respectively.

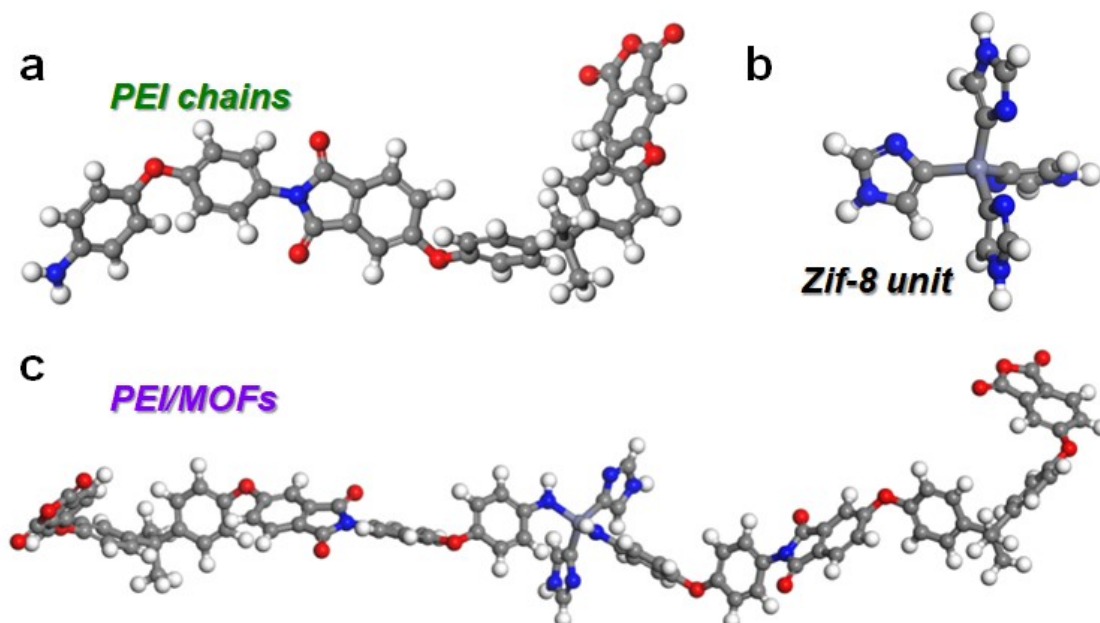


**Figure S18.** The established molecule models of the PEI chain, unit of MOFs and the multisite bonded chain in PEI/MOFs composite.

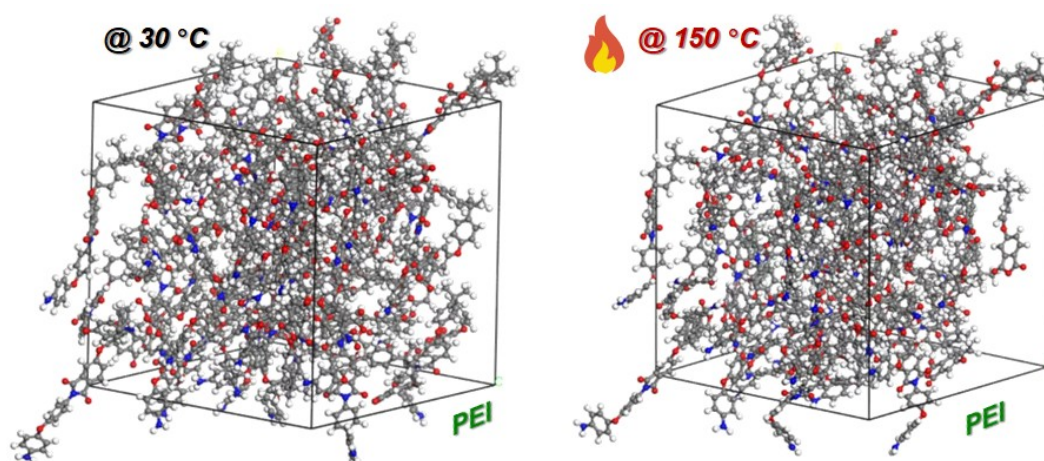


**Figure S19.** Molecular dynamics model of the pristine PEI at room temperature and high temperature.

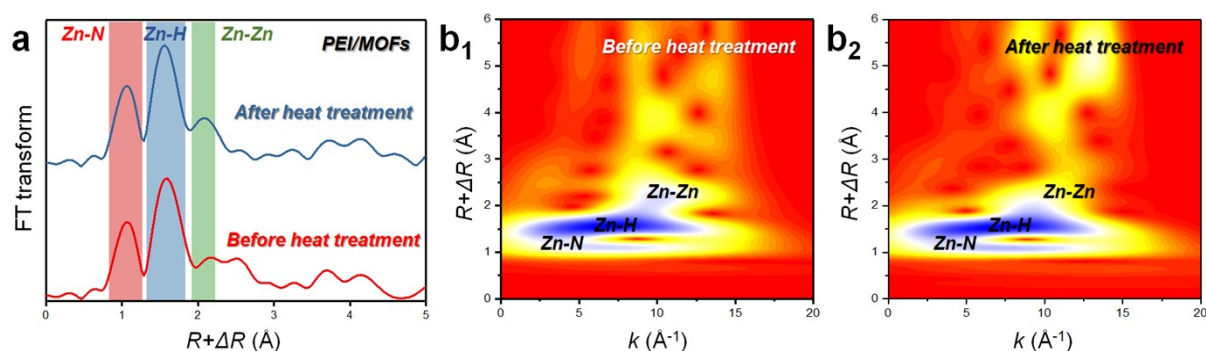


**Figure S20.** (a)  $K$ -edge FT-EXAFS in  $R$  space, (b) wavelet transform analysis for the PEI/MOFs composite before and after the heat treatment.

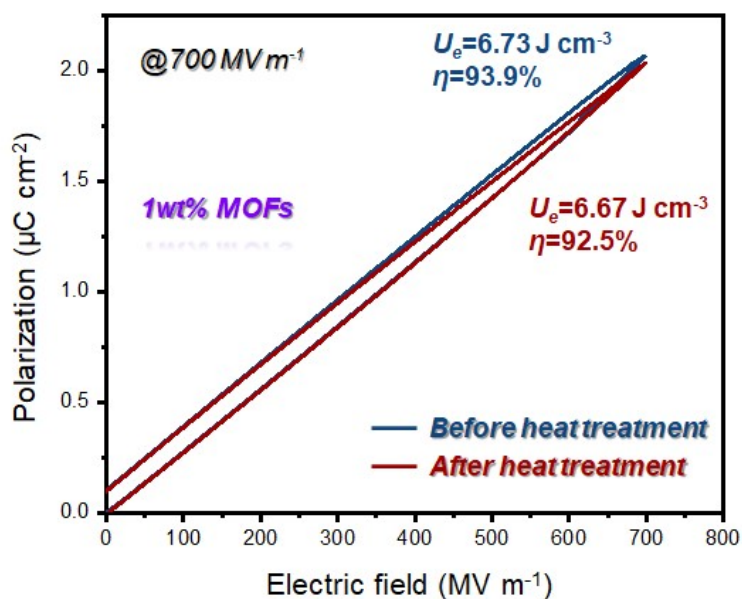


**Figure S21.** *P-E* loops of the PEI/MOFs composite before and after the heat treatment.

*Reference*

- 1 J. Troyano, A. Carné-Sánchez, C. Avci, I. Imaz and D. Maspoch, *Chem. Soc. Rev.*, 2019, **48**, 5534–5546.
- 2 C. Li, J. Liu, K. Zhang, S. Zhang, Y. Lee and T. Li, *Angew. Chemie*, 2021, **133**, 14257–14264.
- 3 Y. Li, J. Yin, Y. Feng, J. Li, H. Zhao, C. Zhu, D. Yue, Y. Liu, B. Su and X. Liu, *Chem. Eng. J.*, , DOI:10.1016/j.cej.2021.132228.
- 4 Q. Shi, Z. Chen, Z. Song, J. Li and J. Dong, *Angew. Chemie*, 2011, **123**, 698–701.